01,13

Anisotropy and delayed relaxation of the anomalous Hall effect in GdFeCo/Ir/GdFeCo synthetic ferrimagnets

© M.V. Bakhmetiev[1], A.D. Talantsev[1], O.V. Koplak[1,2], R.B. Morgunov[1,2]

[1] Federal Research Center for Problems of Chemical Physics and Medical Chemistry of the Russian Academy of Sciences, Chernogolovka, Russia
[2] I.M. Sechenov First Moscow State Medical University, Moscow, Russia

E-mail: bakhmetiev.maxim@gmail.com

Received September 11, 2022
Revised September 11, 2022
Accepted September 24, 2022

In synthetic ferrimagnets with perpendicular anisotropy GdFeCo/Ir/GdFeCo, the dependence of the hysteresis loops of the anomalous Hall resistance and the characteristics of the loops on the angle between the magnetic field and the plane of the sample are analyzed. The part of the anomalous Hall resistance corresponding to the spin-orbit torque has been identified. The field dependences of the resistance are sensitive to switching between the magnetic states of the two-layer ferrimagnet and they reproduce the shapes of the magnetization hysteresis loops, calculated with the interlayer exchange interaction, crystal anisotropy, and Zeeman energies at different angles between the field and sample. A slow (~ 30 min) magnetic relaxation of resistivity hysteresis after reorientation of the sample in magnetic field was found. Specific domain dynamics inherent in two-layer samples was revealed by Kerr microscopy. It was found that slow restoration of the resistivity hysteresis loop is due to domain propagation.

Keywords: spin Hall effect, spin-orbit torque, magnetic relaxation, domain wall dynamics.

DOI: 10.21883/PSS.2023.01.54966.473

1. Introduction

GdFeCo thin films are an extremely interesting object for research in the field of spintronics, since they demonstrate many new effects associated with the possibility of controlling their magnetization by unconventional methods. In the absence of a magnetic field, such films can be magnetized by an electric current [1–3] or by an ultrashort pulse of polarized light [4–7]. These phenomena attach particular importance to the study of these films because the potential for reducing the size of memory elements controlled by an external magnetic field currently seems to be exhausted [8]. Materials of the RE−TM family have been used before as a medium for recording information in magneto-optical disks, including GdFeCo serially used in the production of [9]. However, only its magnetothermal properties were used to record information, so that the remagnetization of the memory element required its heating and cooling. These processes take considerable time and do not meet modern requirements for the speed of writing and reading information. At the same time, subpicosecond laser pulse durations and short electric field pulses are quite achievable. Such effects on the magnetic memory element are recognized as promising for creating devices of the new generation.

The main amount of data on the anomalous Hall effect (AHE) was obtained for heterostructures in which a single Gd layer is surrounded by layers of heavy transition metals (Pt, Ta, etc.) [10–14]. For such samples, it is proved that, in addition to the classical Hall effect, in which the transverse stress linearly depends on the external field, the main mechanism of AHE is the spin-orbit torque (SOT). In the structures Pt/Gd/Pt, Ta/Gd/Pt, etc., the scattering of charge carriers on impurities and defects with spin depends on the direction of magnetization of the ferromagnetic layer [11,15,16]. In addition, the loss of inversion symmetry at the interface leads to another SOT mechanism, which consists in such mixing of the wave functions of the conduction electron subzones, which gives transverse electric polarization. SOT is considered as the most important method of transmitting the spin polarization of conduction electrons to the ions of the ferromagnetic core.

Injection of spin-polarized current into a ferromagnet is an effective way of its remagnetization, replacing the external field [17,18]. Therefore, two-terminal devices are of great interest, in which spin polarization of charge carriers occurs in the first layer of GdFeCo (it can also occur in transition metals Pt, Ir, Ta, etc.), and then this current is injected into the second layer. The transfer of spin angular momentum from the conduction electron to the lattice ion is carried out through the spin-orbit interaction so that the law of conservation of angular momentum in the electron-ion pair is fulfilled. As a result, this process leads to a reversal of those ion spins that were directed against the direction of polarization of the conduction electrons. Therefore, the second ferromagnetic layer changes the direction of magnetization. The spin current generated by the flow of electric current is determined by the expression

$\mathbf{J}_S = (\hbar/2e) \cdot \theta_{SH} \cdot \mathbf{J}_C \times \boldsymbol{\sigma}$, where $\mathbf{J}_S$ and $\mathbf{J}_C$ — spin current and electric current in the sample plane, respectively, $\boldsymbol{\sigma}$ — spin polarization of the current, θ_{SH} — Hall angle characterizing the efficiency of converting electric current into spin current. The mutual orthogonality of the vectors $\mathbf{J}_S$, $\mathbf{J}_C$ and $\boldsymbol{\sigma}$ leads to spin polarization in the plane of the ferromagnetic film.

Both ferromagnetic layers should be located at a small distance (~ 1 nm) in order to prevent spin decoherence of charge carriers. At such distances between ferromagnetic thin films, there is an exchange interaction between them, transmitted by conduction electrons [19]. Such heterostructures are called synthetic ferrimagnets. In them, depending on the spacer t thickness, separating the ferromagnetic layers, an oscillating change in the exchange interaction, its magnitude and sign is observed. It is usually possible to pick up t in such a way that the interlayer exchange interaction has a negative sign (antiferromagnetic), and is comparable in magnitude to the Zeeman interaction of the external field $0.1-1$ kOe with a ferromagnetic layer. In this case, at different thicknesses of ferromagnetic layers, the heterostructure is called a synthetic ferrimagnet, and it is capable of switching by an external magnetic field between four states of magnetization corresponding to different mutual orientation of the magnetizations of the two layers: the state P^+ corresponding to the orientation $\uparrow\uparrow$, state P^- with orientation $\downarrow\downarrow$, state AP^+ with orientation $\uparrow\downarrow$ and the state AP^- with orientation $\downarrow\uparrow$.

In the GdFeCo films, there is another possibility to control spin polarization and magnetization. Change of stoichiometry in samples $Gd_x(Fe\ Co)_y$ leads to variations in the contributions of the rare-earth sublattice and the sublattice of transition metals. The magnetism of the rare earth sublattice is determined by the shell Gd — its $4f$-shell, while the magnetism of the sublattice of transition metals is determined by the $3d$-shells of Fe^{2+} and Co^{2+} ions. The antiferromagnetic interaction of sublattices is determined by the $5d$-electrons of Gd^{3+} ions through the exchange interaction of $4f-5d$ and hybridization of $3d-5d$. The alloy $Gd_x(FeCo)_y$ is a ferrimagnet and has a compensation point, the temperature of which varies significantly (in the range $50-300$ K) depending on the concentrations of x and y. At room temperature, the magnetization of the FeCo sublattice usually dominates, and below the compensation point, the main contribution to magnetization is made by the rare-earth sublattice [20,21]. We can say that the structures considered in our work are „doubly“ ferrimagnets due to ferrimagnetism inside the GdFeCo layers and the ferrimagnetic interaction between them at certain spacer thicknesses t.

A synthetic ferrimagnet is not equivalent to two separate ferromagnetic layers due to the presence of interlayer exchange interaction, which can significantly change the spin-galvanic and magnetic properties of a ferrimagnet [22,23]. In addition to synthetic ferrimagnets, ferromagnet/antiferromagnet structures with the exchange offset [24] provide an opportunity to study the effect of exchange interaction on the Hall effect from neighboring layers. The controlling factors of magnetization reversal of synthetic ferrimagnets are interlayer exchange interaction, magnetocrystalline perpendicular anisotropy and Zeeman interaction with an external magnetic field. The energy balance of these interactions determines the magnetization state of the heterostructure and its electrical conductivity, including, for example, the giant magnetoresistance [8,9]. If the dimensions of a ferrimagnet allow for the existence of a multi-domain structure in it, the domain dynamics turns out to be much more complicated than in a single film, due to the presence and interaction of several types of domains providing slow magnetic relaxation [25] and macroscopic magnetization oscillations [26].

Works in the field of SOT research in synthetic ferrimagnets are quite rare in the literature. This direction is important for the development of two- and multi-terminal magnetic memory devices, and is also of fundamental interest. In particular, it is important to understand how spin-polarized electrons in the spacer, which provide the interlayer exchange interaction, affect the anomalous Hall effect and its dominant part provided by SOT in GdFeCo.

The purpose of this work was to obtain the angular dependence of the anomalous Hall resistance and to compare it with the analytical angular dependence of magnetization in two-layer synthetic ferrimagnets $Gd_{0.25}[Fe_{0.9}Co_{0.1}]_{0.75}$ with perpendicular magnetization. In addition, the aim of the work was to create experimental conditions for observing the slow magnetic relaxation of SOT caused by the restructuring of the domain structure in the heterostructure with a sharp change in the direction of the external magnetic field.

2. Procedure and samples

In experiments, multilayer heterostructures were used Pt (5.6 nm)/Cu (4 nm)/$Gd_{0.25}[Fe_{0.9}Co_{0.1}]_{0.75}$ (5.2 nm)/Ir (0.6 nm)/$Gd_{0.25}$ $[Fe_{0.9}Co_{0.1}]_{0.75}$ (4.2 nm)/Cu (5.6 nm)/Ta (5 nm), sprayed by a magnetron onto a Si/SiO_2 substrate with a thermally enhanced oxide layer 100 nm thick to provide insulation and prevent leakage of electric currents (Fig. 1, *a*).

The substrate was obtained in pure nitrogen and etched with argon plasma with a power of 50 W at a pressure of $1 \cdot 10^{-2}$ mbar during 5 min. During spraying, the sample was rotated at a frequency of $\sim 10-30$ rpm. A buffer layer of tantalum was sprayed onto the surface of a silicon substrate, and the Pt layer served as a cover layer. The copper layer improved the perpendicular magnetic anisotropy.

Distributions of chemical elements in the cross section of the sample were obtained using a high-resolution JEOL microscope (HR TEM) with an X-ray energy dispersion (EDX) prefix at an accelerating voltage of 200 kW (Fig. 1, *b*). The upper and lower layers of GdFeCo, as well

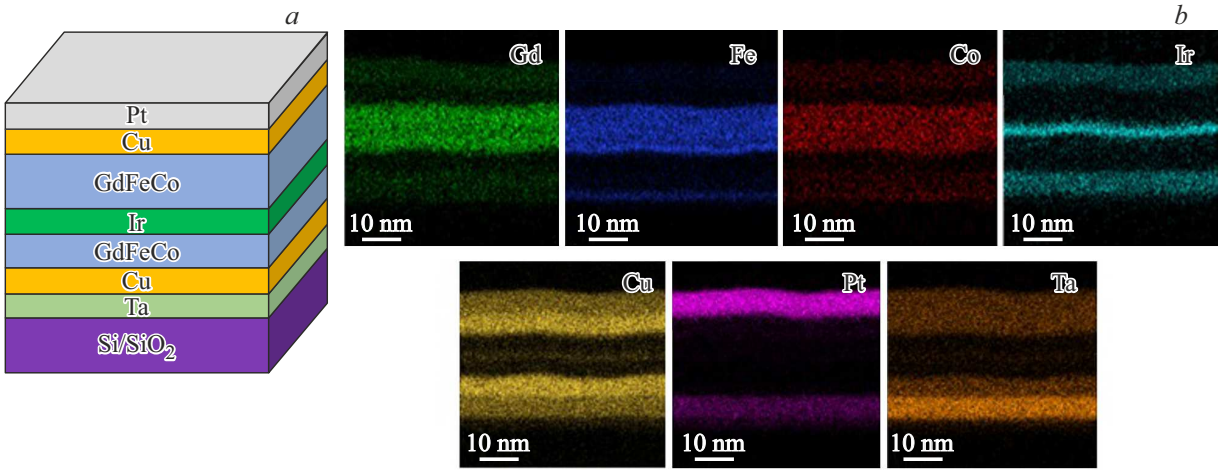

Figure 1. *a* — schematic representation of the heterostructure Pt (5.6 nm)/Cu (4 nm)/$Gd_{0.25}[Fe_{0.9}Co_{0.1}]_{0.75}$ (5.2 nm)/Ir (0.6 nm)/$Gd_{0.25}[Fe_{0.9}Co_{0.1}]_{0.75}$ (4.2 nm)/Cu (5.6 nm)/Ta (5 nm). *b* — the image obtained by the EDX method of the distribution of chemical elements in the cross-section of the sample.

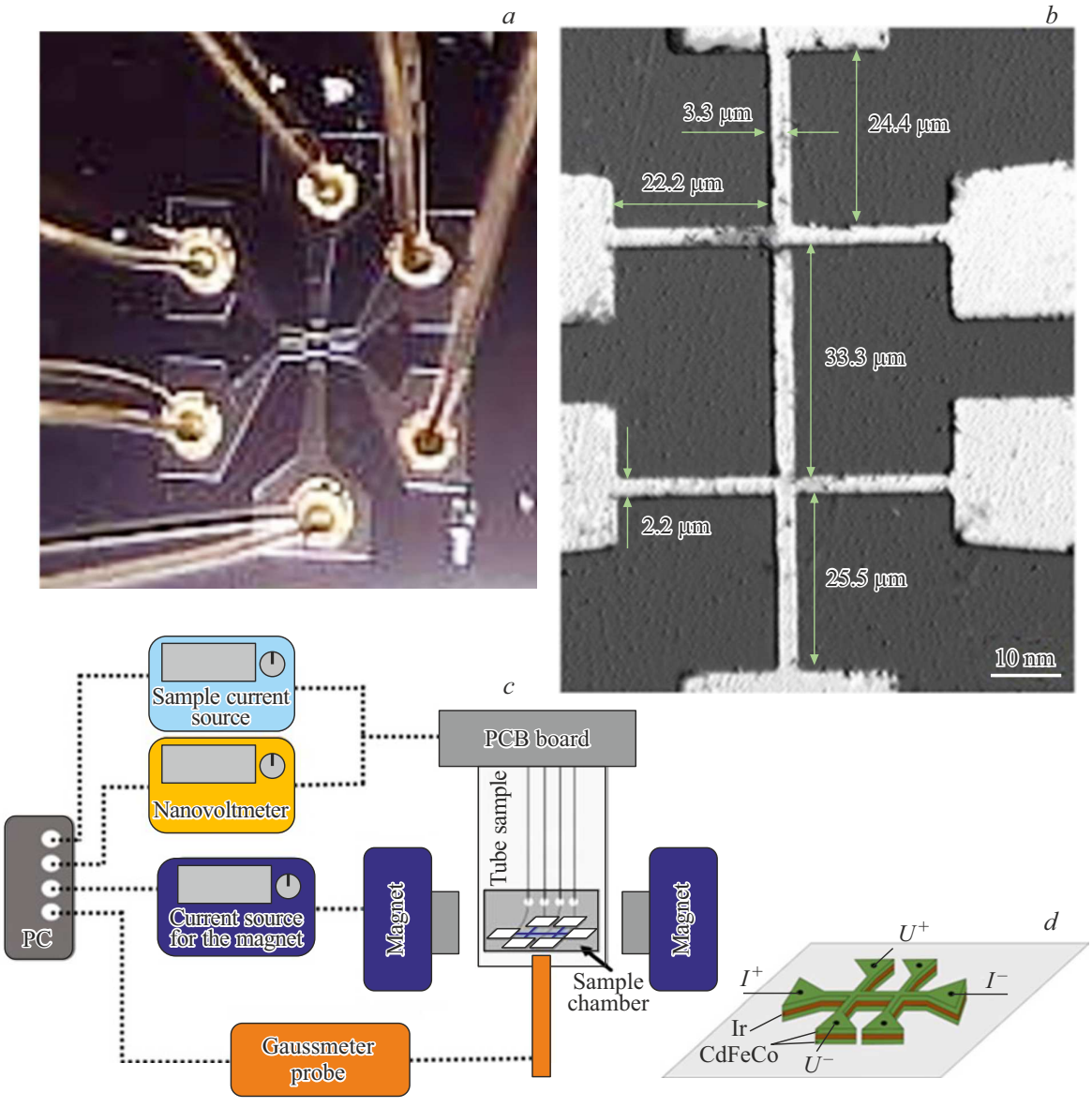

Figure 2. *a* — optical image of a patterned sample with gold contacts; *b* — optical image of the Hall bridge; *c* — diagram of an experimental setup for measuring the Hall effect; *d* — electrical wiring diagram of contacts for measuring the Hall effect on direct current.

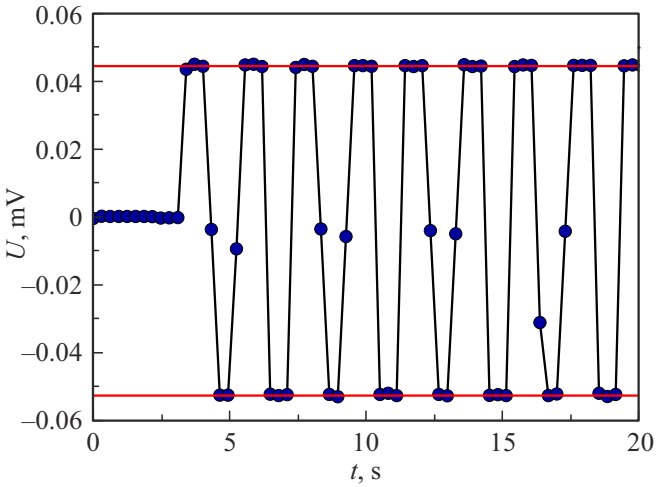

Figure 3. The time dependence of the Hall voltage caused by rectangular current pulses with amplitudes −1 and 1 mA duration 1 s.

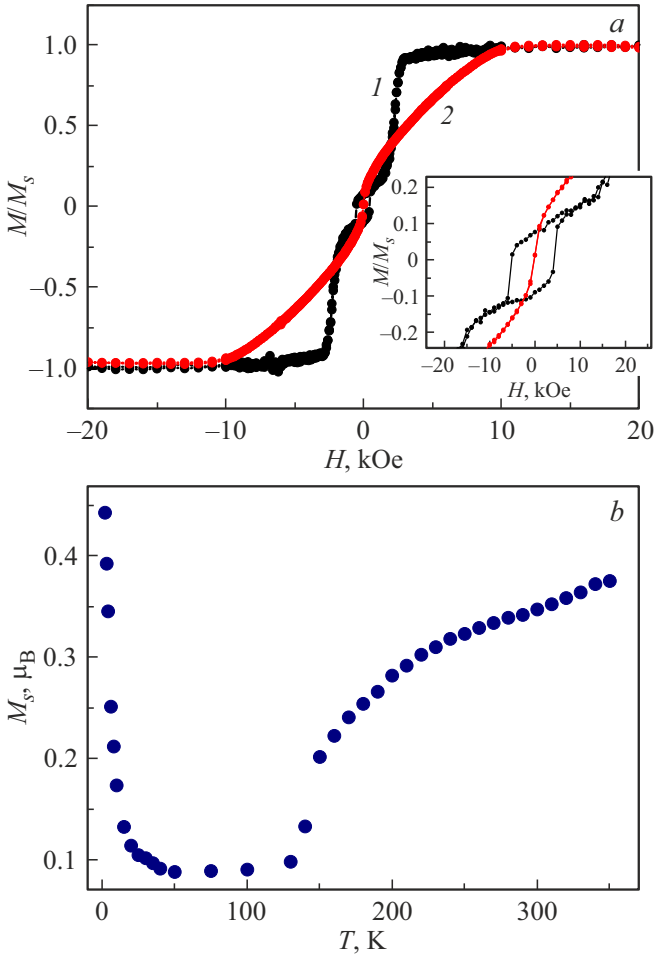

Figure 4. *a* — field dependences of the reduced magnetization at 300 K in a magnetic field perpendicular (*1*) and parallel (*2*) to the sample plane. *b* — temperature dependence of saturation magnetization per one formula unit $Gd_{0.25}[Fe_{0.9}Co_{0.1}]_{0.75}$, obtained in a magnetic field 1 T, perpendicular to the plane of the sample.

as the Ir layer, were in an amorphous state. Both layers of copper and the upper layer of Pt were crystallized and had a texture (111) corresponding to the predominant grain growth along the crystallographic direction [111]. The relative intensities for Gd, Fe and Co atoms corresponded to the atomic stoichiometry of the sample $Gd_{0.25}[Fe_{0.9}Co_{0.1}]_{0.75}$, which is close to the composition of the target.

Optical lithography was used to obtain a cross-shaped pattern (Fig. 2, *a* and *b*), providing connection with gold contacts.

The measurement scheme of the transverse voltage at direct current with a given value is shown in Fig. 2, *c*. Keithley 6220, Keithley 2182A and PCE-MFM 3000 devices were used, automated for computer data recording and interactive control of them and magnetic field scanning. The connecting diagram of the contacts to the sample is shown in Fig. 2, *d*. An external magnetic field during electrical measurements was created using an Abbess Instruments electromagnet.

Since the experiments included sharp changes in the direction of the magnetic field, control measurements were performed in which the transient mode and the minimum duration of the current pulse were studied, ensuring the correct shape of the corresponding voltage pulse of the classical Hall effect (Fig. 3). The time constant of the complex of electrophysical measurements was ~ 1 s.

The dynamics of the domain walls and hysteresis loops were recorded in the field range −2.7−2.7 kOe at room temperature in a Durham NanoMOKE3 Kerr microscope with polar geometry. A laser spot with a diameter of 5 μm was focused on one of the petals of the patterned sample. The field sweep rate during the recording of hysteresis loops was 1080 Oe/s.

Magnetic measurements of a solid sample without a cross-shaped pattern at temperatures of 2−360 K were performed using a Quantum Design MPMS XL SQUID magnetometer.

3. Experimental results

From the measurement of magnetic hysteresis loops in a magnetic field perpendicular and parallel to the sample plane, it was found that at temperatures $T > 100$ K, the axis of light magnetization is perpendicular to the sample plane (Fig. 4, *a*). The magnetic moment in the saturation state M_S at 300 K is 132 emu/cm^3, which is typical for an amorphous alloy with the composition $[Fe_{0.9}Co_{0.1}]_{0.75}$ [25] and in terms of one formula unit is 0.25 μB.

The temperature dependence of saturation magnetization obtained in a strong magnetic field (1 T) demonstrates a strong drop in magnetization during cooling from 350 to 70 K, and its further increase during cooling from 70 to 2 K (Fig. 4, *b*). Such dependence is typical for a ferrimagnet with two sublattices and a compensation point at 60−80 K. From measurements of the X-ray magnetic circular dichroism (XMCD), it is known that

in the high temperature region the contribution of Fe prevails, and at low temperatures — the contribution of Gd [25–28]. The flat bottom in the minimum of the dependence $M_S(T)$ does not allow to accurately determine the compensation temperature. This may be due to a significant variation in the values of this temperature in different parts of the film exposed to mechanical stresses.

A Kerr microscope was used to study the switching between the states P^+, P^-, AP^+ and AP^-. The hysteresis loop was recorded in a magnetic field with a sweep velocity of 1080 Oe/s, perpendicular to the sample plane,

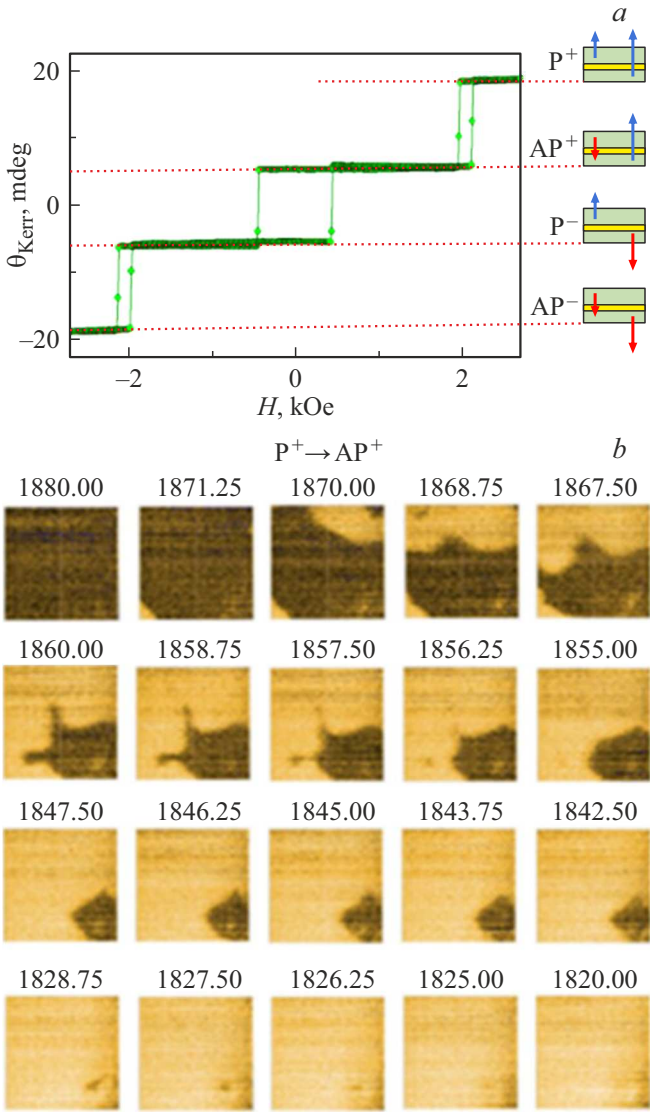

Figure 5. *a* — a hysteresis loop recorded using a Kerr microscope at a field sweep rate of 1080 Oe/s and a temperature of 300 K. The field is perpendicular to the sample. Different magnetic states are shown on the right. The arrows show the directions of magnetization of the GdFeCo layers in the states P^+, P^-, AP^+ and AP^-. *b* — the domain dynamics accompanying the transition $P^+ \leftrightarrow AP^+$ when an external magnetic field is applied; for each image, the field strength in Oe is indicated.

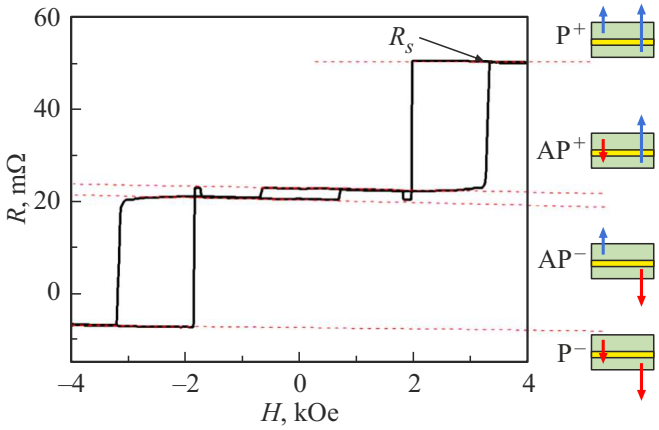

Figure 6. Dependence of the Hall resistance R on the magnetic field at electric current $I = 1$ mA at 300 K. Different magnetic states are shown on the right.

at $T = 300$ K (Fig. 5, *a*). Switching $P^+ \rightarrow AP^+$ occurs at $H = 1.8$ kOe, and reverse switching $AP^+ \rightarrow P^+$ is observed at $H = 2.0$ kOe. Transitions $AP^+ \rightarrow AP^-$ and $AP^- \rightarrow AP^+$ occur in the magnetic fields $H = \pm 450$ Oe. An example of a domain structure in the transition $P^+ \rightarrow AP^+$ is shown in Fig. 5, *b*.

Since a change in the anomalous Hall resistance reproduces a change in the magnetization of the sample, another way to record the hysteresis loop was to use not magnetization, but the electrical resistance of the R heterostructure as a response to an external field. Dependence of electrical resistance R from the external field perpendicular to the sample, after subtracting the classical Hall effect linearly dependent on the field, is shown in Fig. 6. Figure 6 on the right shows the magnetization of the heterostructure layers in the states P^+, P^-, AP^+ and AP^- corresponding to the horizontal sections of the resistance hysteresis loop.

Since the scanning speed in the Kerr microscope and in the Hall voltage measurement unit was higher than in the SQUID magnetometer, the critical fields of transitions between states were slightly higher: ± 3.2 kOe with increasing field and ± 2 kOe with decreasing field for transitions $P^+ \leftrightarrow AP^+$ and $P^- \leftrightarrow AP^-$, respectively (see lateral hysteresis loops in Fig. 6). The central hysteresis loop $R(H)$ with switching fields ± 650 Oe corresponds to the transitions $AP^+ \leftrightarrow AP^-$. Different thicknesses of GdFeCo layers lead to different total magnetization in the states AP^+ and AP^-.

We have obtained hysteresis loops $R(H)$ at different angles θ between the magnetic field and the normal to the sample $\mathbf{n}$ (Fig. 7). The linear contribution due to the classical Hall effect was subtracted from all the dependencies shown in Fig. 7. A change in the angle of θ leads to a significant change in the shape of the hysteresis loops and a shift in the switching fields.

The sharpest switching between the states AR^+ and AR^- is observed at the angles $\theta = 0°$ and $\theta = 180°$. If the

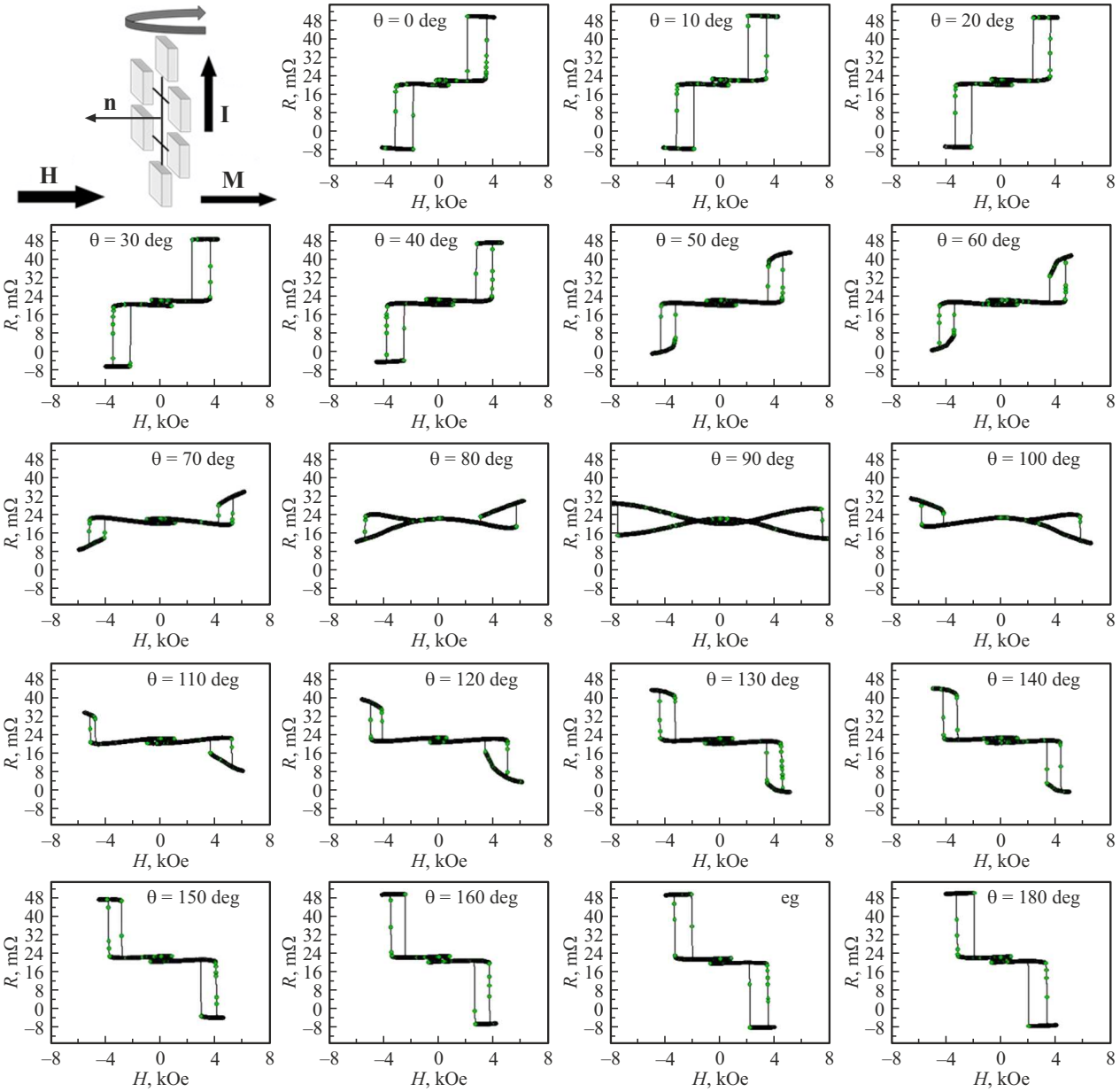

Figure 7. The dependences of the SOT voltage on the magnetic field for different orientations of the field with respect to the normal to the sample plane at a temperature of 300 K and a current of 1,mA, as well as the rotation scheme of the sample when measuring the angular dependence of the resistance hysteresis (the mutual orientations of magnetization **M**, electric current **I**, the magnetic field **H** and the normal vector to the sample plane **n**).

vectors **H** and **M** are perpendicular ($\theta = 90°$), there is no switching on the central hysteresis loop.

In thin films of small linear sizes (~ 10 nm) there are no domains, and the magnetization can switch in a short time ~ 1 ps [28]. In the films and heterostructures of macroscopic dimensions (~ 1 mm), admitting the existence of domains, long-term magnetic relaxation [25] can be observed. This is due to the fact that in structures with two exchange-bound ferromagnetic layers, there are four types of domains with different mutual orientations of magnetization of thick and thin layers. In the general case, the sample may contain domains with magnetizations of the type P^+, P^-, AP^+ and AP^-. Interaction and mutual absorption of such domains can be a long process with a time constant of tens of minutes [25]. Since the SOT depends on the magnetization of each layer and the orientation of the magnetization with respect to the electric current, it can be assumed that the measurement of the Hall voltage and its part of the SOT can also relax over time, following the dynamics of the domain walls. To detect such a phenomenon, the sample was first magnetized by a field 1 T in the sample plane. Then the field was turned off and the

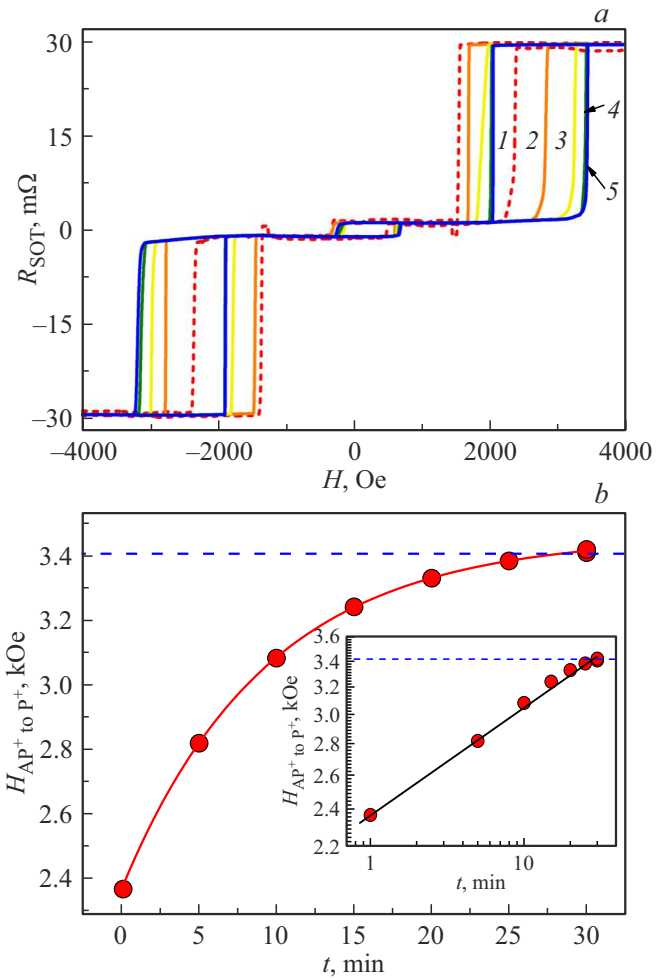

Figure 8. *a* — dependences of the SOT resistance on the magnetic field, measured in 1 (*1*), 5 (it2), 15 (it3), and 30 min (*4*) after rotation of the sample from a position with the orientation of the field along the plane to a position with the orientation of the field perpendicular to the plane. *b* — dependence on the time of the switching field between the states AP^+ and P^+, established by the loops of magnetic hysteresis $R(H)$, measured at different times after the reorientation of the field 1 T relative to the sample. Solid line — approximation by exponential function. Dotted line — switching field in a sample not magnetized in the plane. The insert shows the same dependence in semi-logarithmic coordinates.

sample rotated by 90° for ~ 10 s. Further, the resistance hysteresis loop was measured when the field was oriented perpendicular to the sample plane. The first measurement made 1 min after the sample rotation showed a hysteresis loop with critical switching fields that significantly differed from the fields obtained in the demagnetized (control) sample. If the pause between the rotation of the sample and the measurement of the hysteresis loop increased, the switching fields changed, gradually approaching their initial value in the control sample (Fig. 8, *a*).

To quantify this relaxation, a time dependence of the critical switching field $H_{AP^+\to P^+}(t)$ was constructed from the state AP^+ to the state P^+ (fig. 8, *b*). Approximation of the dependence $H_{AP^+\to P^+}(t)$ by an exponential function allowed us to determine the relaxation time constant 10 min, which turned out to be significantly less than the time constant of the complex of electrophysical measurements ~ 1 s. During ~ 30 min, the values of the switching fields and the position of the lateral hysteresis loop were completely restored to the values in the original demagnetized sample. It follows from the results obtained that the switching field detected by the Hall voltage is determined by the slow dynamics of the domain walls, previously studied in detail in two-layer samples with perpendicular anisotropy.

4. Discussion of experimental results

In general case, the Hall resistance in GdFeCo/Ir structures consists of contributions of the classical Hall effect R_{OHE} and the anomalous Hall effect R_{AHE}, which, in turn, consists of two components: the spin Hall effect R_{SHE} and the planar Hall effect R_{PHE} (anisotropic magnetoresistance). As a result, the Hall resistance as a function of the angle between the field and the normal to the sample plane θ and the angle between the electric current and the external field φ, can be written as:

$$R = R_{OHE} + R_{AHE}\cos\theta + R_{PHE}\sin^2\theta\sin 2\varphi. \qquad (1)$$

It has been shown that, although the injection of spin current is possible from one ferromagnetic layer to another as a result of the action of the planar Hall effect (PHE) [29,30], this mechanism does not lead to the emergence of SOT in a system of two ferromagnetic layers. The planar Hall effect can only cause spin polarization perpendicular to the plane of the sample [31]. To observe the maximum value of PHE, the angle φ between the electric current

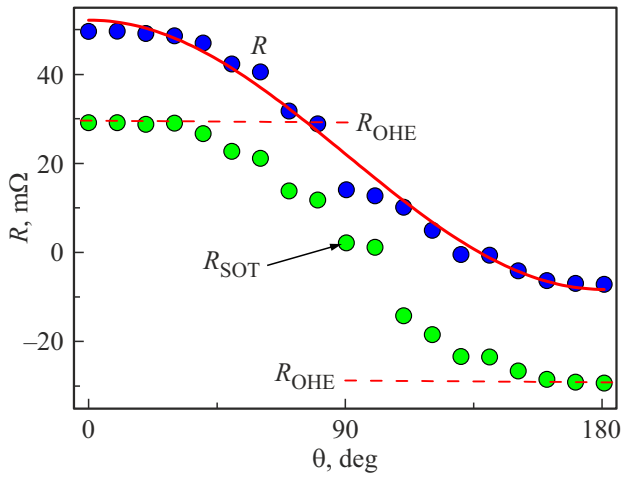

Figure 9. The angular dependence of the total Hall resistance in the saturation state of magnetization P^+ (blue symbols) and the angular dependence SOT after subtracting the contribution of the classical Hall effect OHE. The OHE contribution is shown by dotted lines. The approximation by the formula (1) is shown by a solid line.

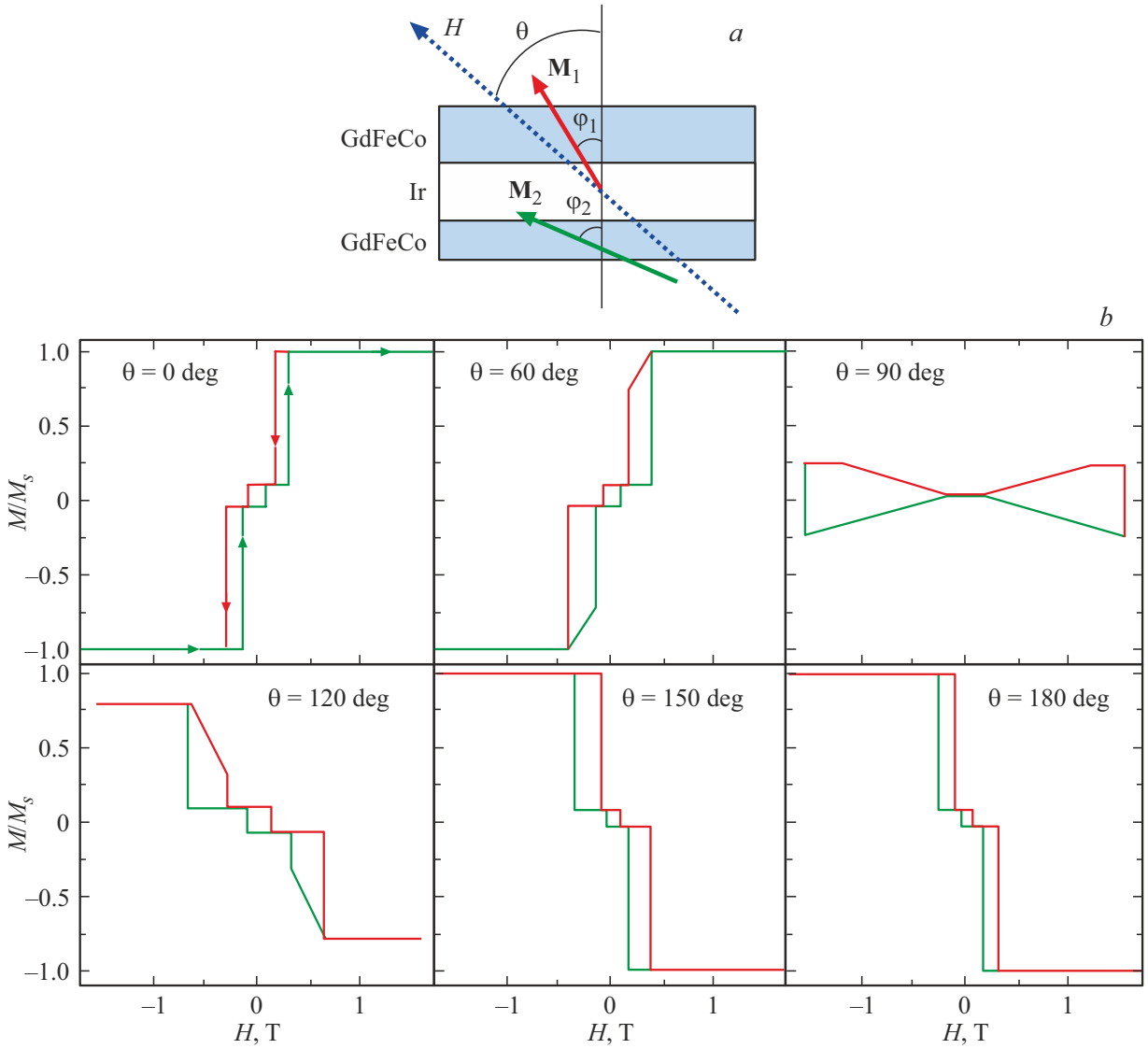

Figure 10. *a* — sample diagram with the directions of magnetization of the layers $\mathbf{M}_1$ and $\mathbf{M}_2$, the external field H and the corresponding angles with the normal. *b* — are calculated angular dependences of the magnetization normalized to saturation magnetization at different angles between the field and the normal line θ.

and the external field must be 0°, since the electric current is parallel to the magnetic moment of the layer $J_{\text{PHE}} = \Delta\sigma_{\text{AMR}}(\mathbf{m} \cdot \mathbf{E})\mathbf{m}$ [32,33], where $\mathbf{E}$ — is the applied field, $\Delta\sigma_{\text{AMR}}$ is the anisotropic part of the conductivity. In our experiments $\varphi = 90°$, so that the third term in the sum (1) is zero. The spin Hall effect, on the contrary, does not depend on the angle φ, but it depends on the angle θ, varied in our experiments.

A series of resistive hysteresis loops $R(H)$ (Fig. 7) allowed us to construct the angular dependence of the resistance of the heterostructure in the state of magnetic saturation P^+ (Fig. 9). In Fig. 9, the approximation of the angular dependence of the Hall resistance (blue symbols) by the expression (1) is shown by a solid line. The angular dependence of the SOT contribution after the OHE subtraction is shown in green symbols. This part was calculated using the formula [34]:

$$R_{\text{SOT}} \cos\theta = \frac{R(H) - R(-H)}{2}. \qquad (2)$$

The OHE contribution is shown by a dotted line. The approximation leads to the values $R_{\text{OHE}} = 22\,\text{m}\Omega$, $R_{\text{SOT}} = 30\,\text{m}\Omega$, similar to the values obtained in [34] for a single-layer sample.

Since the Pt, Cu, Ir layers act as a shunt, changing the resistance of the sample, we calculated the proportion of current flowing through the GdFeCo layer. To do this, we used the known resistivity of metals at room temperature $\rho_{\text{GdFeCo}} = 1.85\,\mu\Omega \cdot \text{cm}$ [35], $\rho_{\text{Ir}} = 4.74 \cdot 10^{-8}\,\Omega \cdot \text{cm}$ [36], $\rho_{\text{Pt}} = 4.74 \cdot 10^{-7}\,\Omega \cdot \text{cm}$ [37], $\rho_{\text{Cu}} = 1.68 \cdot 10^{-8}\,\Omega \cdot \text{cm}$ [38]. Simple calculations gave a shunt coefficient $\xi_{\text{GdFeCo}} = 0.42$, taking into account which

the values of the Hall components of the resistance are equal $R_{\mathrm{OHE}} = 31.2\,\mathrm{m\Omega}$, $R_{\mathrm{SOT}} = 42.6\,\mathrm{m\Omega}$.

The simulation of magnetization hysteresis loops at different directions of the magnetic field was carried out by minimizing the sum of the energy of the Zeeman interaction, the anisotropy energy of each of the layers and the exchange energy of the interaction of the layers [39]:

$$E_{tot} = -t_1 M_1 H\cos(\varphi - \varphi_1) - t_2 M_2 H\cos(\theta - \varphi_2) - K_{eff1}\cos^2\varphi_1 - K_{eff2}\cos^2\varphi_2 - J_{ex}\cos(\varphi_1 - \varphi_2). \quad (3)$$

where t_1 and t_2 — the thicknesses of the GdFeCo layers, M_1 and M_2 — their magnetization, φ_1 and φ_2 — the angles between the magnetizations and the external field H (Fig. 10, *a*), K_{eff1} and K_{eff2} — the constants of effective anisotropy GdFeCo layers, J_{ex} — interlayer exchange interaction. The similarity of the resistance hysteresis (Fig. 7) with the magnetic hysteresis at the corresponding angles between the field and the sample (Fig. 10, *b*) means that the change in the resistance corresponding to SOT reproduces the change in the projection of the total magnetization of the two layers of the field to the normal to the sample.

5. Conclusions

1. Analysis of the angular dependence of the Hall effect in synthetic GdFeCo/Ir/GdFeCo ferrimagnets allowed us to separate the contributions of the classical Hall effect $R_{\mathrm{OHE}} = 22\,\mathrm{m\Omega}$ and the anomalous Hall effect associated with spin-orbit torque, $R_{\mathrm{SOT}} = 30\,\mathrm{m\Omega}$ at room temperature exceeding the compensation temperature of the magnetization of the sublattices ($\sim 60-70\,\mathrm{K}$).

2. Modeling of the field dependence of the magnetization of a two-layer GdFeCo sample yields magnetic hysteresis loops similar to those observed when measuring the Hall resistance hysteresis.

3. A rapid change in the orientation of the magnetic field from the orientation in the plane of the sample to the orientation perpendicular to the sample causes a slow relaxation of the part of the Hall stress corresponding to the spin-orbit torque. The long-term relaxation of this voltage ($\sim 30\,\mathrm{min}$) is associated with domain expansion.

Acknowledgments

The authors are grateful to Prof. S. Mangin for samples and useful discussions.

Funding

The work was carried out as part of the thematic map of the Federal Research Center for Problems of Chemical Physics and Medical Chemistry of the RAS AAAA-A19-119092390079-8.

Conflict of interest

The authors declare that they have no conflict of interest.

References

[1] N. Roschewsky, T. Matsumura, S. Cheema, F. Hellman, T. Kato, S. Iwata, S. Salahuddin. Appl. Phys. Lett. **109**, 112403 (2016).
[2] N.T. Hai, I. Kindiak, V. Yurlov, R.C. Bhatt, C.-M. Liao, L.-X. Ye, T.-H. Wu, K.A. Zvezdin, J.-C. Wu. AIP Adv. **10**, 105202 (2020).
[3] T.H. Pham, S.-G. Je, P. Vallobra, T. Fache, D. Lacour, G. Malinowski, M.C. Cyrille, G. Gaudin, O. Boulle, M. Hehn, J.-C. Rojas-Sanchez, S. Mangin. Phys. Rev. Appl. **9**, 064032 (2018).
[4] Y. Xu, M. Hehn, W. Zhao, X. Lin, G. Malinowski, S. Mangin. Phys. Rev. B **100**, 064424 (2019).
[5] J. Gorchon, R.B. Wilson, Y. Yang, A. Pattabi, J.Y. Chen, L. He, J.P. Wang, M. Li, J. Bokor. Phys. Rev. B **94**, 184406 (2016).
[6] S. Savoini, R. Medapalli, B. Koene, A.R. Khorsand, L.L. Guyader, L. Duo, M. Finazzi, A. Tsukamoto, A. Itoh, F. Nolting, A. Kirilyuk, A.V. Kimel, T. Rasing. Phys. Rev. B **86**, 140404(R) (2012).
[7] Y. Hashimoto, A.R. Khorsand, M. Savoini, B. Koene, D. Bossini, A. Tsukamoto, A. Itoh, Y. Ohtsuka, K. Aoshima, A.V. Kimel, A. Kirilyuk, T. Rasing. Rev. Sci. Instrum. **85**, 063702 (2014).
[8] S. Tehrani, J.M. Slaughter, E. Chen, M. Durlam, J. Shi. IEEE Trans. Magn. **35**, 2814 (1999).
[9] Q. Shao, P. Li, L. Liu, H. Yang, S. Fukami, A. Razavi, H. Wu, K. Wang, F. Freimuth, Y. Mokrousov, M.D. Stiles, S. Emori, A. Hoffmann, J. Akerman, K. Roy, J.-P. Wang, S.-H. Yang, K. Garello, W. Zhang. IEEE Trans. Magn. **57**, 800439 (2021).
[10] W. Zhou, T. Seki, T. Kubota, G.E.W. Bauer, K. Takanashi. Phys. Rev. Mater. **2**, 094404 (2018).
[11] L. Helmich, M. Bartke, N. Teichert, B. Schleicher, S. Fahler, A. Hutten. AIP Adv. **7**, 056429 (2017).
[12] H. Brune, P. Gambardella. Surf. Sci. **603**, 1812 (2009).
[13] R.J. Gambino, T.R. McGuire, K. Fukamichi. J. Appl. Phys. **52**, 2190 (1981).
[14] T.R. McGuire, R.J. Gambino. J. Appl. Phys. **50**, 7653 (1979).
[15] K. Takanashi, H. Kurokawa, H. Fujimori. Appl. Phys. Lett. **63**, 1585 (1993).
[16] K. Takanashi, M. Ohba, H. Kurokawa, H. Fujimori. IEEE Trans. Magn. **9**, 164 (1994).
[17] J. Sinova, S.O. Valenzuela, J. Wunderlich, C.H. Back, T. Jungwirth. Rev. Mod. Phys. **87**, 1213 (2015).
[18] T. Kimura, Y. Otani, T. Sato, S. Takahashi, S. Maekawa. Phys. Rev. Lett. **98**, 156601 (2006).
[19] S.S.P. Parkin. Phys. Rev. Lett. **67**, 3598 (1991).
[20] W.S. Ham, S. Kim, D.H. Kim, K.-J. Kim, T. Okuno, H. Yoshikawa, A. Tsukamoto, T. Moriyama, T. Ono. Appl. Phys. Lett. **110**, 242405 (2017).
[21] K.-J. Kim, S.K. Kim, Y. Hirata, S.-H. Oh, T. Tono, D.-H. Kim, T. Okuno, W.S. Ham, S. Kim, G. Go, Y. Tserkovnyak, A. Tsukamoto, T. Moriyama, K.-J. Lee, T. Ono. Nature Mater. **16**, 1187 (2017).
[22] S.D. Ganichev, E.L. Ivchenko, V.V. Bel'Kov, S.A. Tarasenko, M. Sollinger, D. Weiss, W. Wegscheider, W. Prettl. Nature **417**, 153 (2002).

[23] K. Ando, S. Takahashi, K. Harii, K. Sasage, J. Ieda, S. Maekawa, E. Saitoh. Phys. Rev. Lett. **101**, 036601 (2008).
[24] H. Wu, C.H. Wan, Z.H. Yuan, X. Zhang, J. Jiang, Q.T. Zhang, Z.C. Wen, X.F. Han. Phys. Rev. B **92**, 054404 (2015).
[25] [25]R.B. Morgunov, A.V. Yurov, V.A. Yurov, A.D. Talantsev, A.I. Bezverhnii, O.V. Koplak. Phys. Rev. B **100**, 144407 (2019).
[26] O. Koplak, A. Talantsev, Y. Lu, A. Hamadeh, P. Pirro, T. Hauet, R. Morgunov, S. Mangin. J. Magn. Magn. Mater. **433**, 91 (2017).
U. Atxitia, T.A. Ostler. Appl. Phys. Lett. **113**, 062402 (2018).
[27] J. Sim, J.-H. Lee, S.-K. Kim. J. Magn. Magn. Mater. **542**, 168583 (2022).
[28] A. Kirilyuk, A.V. Kimel, T. Rasing. Rep. Prog. Phys. **76**, 026501 (2013).
[29] J.D. Gibbons, D. MacNeill, R.A. Buhrman, D.C. Ralph. Phys. Rev. Appl. **9**, 064033 (2018).
[30] S. Park, S. Lee, K.J. Lee, S.J. Park, P. Chongthanaphisut, J. Jang, S. Lee, X. Liu, M. Dobrowolska, J.K. Furdyna. Sci. Rep. **11**, 10263 (2021).
[31] C. Safranski, E.A. Montoya, I.N. Krivorotov. Nat. Nanotechnol. **14**, 27 (2019).
[32] T. Taniguchi, J. Grollier, M.D. Stiles. Phys. Rev. Appl. **3**, 044001 (2015).
[33] T. McGuire, R. Potter. IEEE Trans. Magn. **11**, 1018 (1975).
[34] S. Yang, J. Choi, J. Shin, K. Yoon, J. Yang, J.P. Hong. Sci. Rep. **8**, 11065 (2018).
[35] G.K. Reeves, M.W. Lawn, R.G. Elliman. J. Vac. Sci. Technol. A **10**, 3203 (1992).
[36] J.S. Agustsson, U.B. Arnalds, A.S. Ingason, K.B. Gylfason, K. Johnsen, S. Olafsson, J.T. Gudmundsson. Appl. Surf. Sci. **254**, 7356 (2008).
[37] A. Javed, J.-B. Sun. Appl. Surf. Sci. **257**, 1211 (2010).
[38] J. Gogl, J. Vancea, H. Hoffmann. J. Phys.: Condens. Matter **2**, 1795 (1990).
[39] H.S. Tarazona, W. Alayo, C.V. Landauro, J. Quispe-Marcatoma. J. Magn. Magn. Mater. **446**, 44 (2018).